Dissection of Human Tropoelastin: Exon-By-Exon Chemical Synthesis and Related Conformational Studies

ARTICLE *in* BIOCHEMISTRY · DECEMBER 2003

Impact Factor: 3.02 · DOI: 10.1021/bi034837t · Source: PubMed

3 AUTHORS, INCLUDING:

Brigida Bochicchio
Università degli Studi della Basilicata
56 PUBLICATIONS **1,054** CITATIONS
SEE PROFILE

Antonietta Pepe
Università degli Studi della Basilicata
67 PUBLICATIONS **889** CITATIONS
SEE PROFILE

Dissection of Human Tropoelastin: Exon-By-Exon Chemical Synthesis and Related Conformational Studies†

Antonio M. Tamburro,* Brigida Bochicchio, and Antonietta Pepe

Department of Chemistry, Università della Basilicata, Via N. Sauro 85, 85100 Potenza, Italy

Received May 20, 2003; Revised Manuscript Received August 1, 2003

ABSTRACT: Polypeptide sequences encoding the single exons of human tropoelastin were synthesized and their conformations were studied in different solvents and at different temperatures by CD and ^{1}H NMR. The results demonstrated the presence of labile conformations such as poly-proline II helix (PPII) and β-turns whose stability is strongly dependent on the microenvironment. Stable, periodic structures, such as α-helices, are only present in the poly-alanine cross-linking domains. These findings give a strong experimental basis to the understanding of the molecular mechanism of elasticity of elastin. In particular, they strongly support the description of the native relaxed state of the protein in terms of trans-conformational equilibria between extended and folded structures as previously proposed [Debelle, L., and Tamburro, A. M. (1999) *Int. J. Biochem. Cell. Biol. 31*, 261−272].

Resilience and elastic recoil are properties conferred on all vertebrate elastic tissues by elastic fibers (*1*, *2*). These complex extracellular matrix biopolymers are composed of two distinct morphological entities. The amorphous component is made up of insoluble elastin, a highly cross-linked and hydrophobic protein assembled from a soluble precursor protein called tropoelastin. The microfibrillar component of elastic fibers is composed of several glycoproteins, of which the best known are the fibrillins (fibrillin-1 and fibrillin-2) (*3*, *4*). Elastic microfibrils are thought to provide a three-dimensional scaffold for the assembly of elastin during the formation of elastic fibers, while it is insoluble elastin that confers to elastic fibers the property of elastic recoil. The elastic properties of elastin have been explained in terms of entropic components, with questions still remaining about whether the basic mechanism is compatible with the classical theory of rubber elasticity (*5*). A better understanding of structure−function relationships in terms of the protein's elastic properties remains an important goal in elastin biology. Not only will this provide mechanistic insight into how elastin functions, but may suggest a general mechanism for other elastomeric proteins such as spider silk elastic proteins, glutenin, abductin, etc. (*6*). Furthermore, a complete elucidation of elastin's elasticity is essential for the design of proper biopolymers and biomaterials based on elastomeric proteins (*7*).

The unusual physical properties of elastin have precluded a thorough analysis of the protein's three-dimensional structure at atomic resolution. Mature, cross-linked elastin does not crystallize (as expected for rubber-like material), thereby preventing structural analysis by X-ray diffraction. Similarly, its extreme insolubility in common solvents precludes the use of classical spectroscopic techniques. For these reasons, past studies were confined to the use of soluble derivatives, such as α-elastin (*8*) and k-elastin (*9*), and to short synthetic peptides corresponding to repeating sequences (*10*−*13*). In some cases, peptides containing polymeric repeats of variable molecular weight were also studied (*14*−*18*). Together, these studies provided evidence for the presence in the elastin molecule of β-turns (type I, type II, and type VIII), whose stability depends on both sequence and microenvironment. As a general rule, the turns are characterized by having PG, GG, and YG (Y = L, V) at the corners. In addition, Tamburro and co-workers (*19*) found that appreciable amounts of poly-L-proline II left-handed helix (PPII)[1] also contribute to the overall three-dimensional architecture of elastin.

The recent availability of full-length tropoelastin obtained by recombinant DNA techniques provides for the first time an opportunity to explore domain structure within the intact protein (*20*, *21*). Limited CD (*22*) and Raman (*23*) spectra studies of this molecule have confirmed the presence of β-turns and show the presence of α-helix (currently attributed to the poly-alanine cross-linking regions) and possibly some beta strands. A more detailed study of the solution structure of tropoelastin, however, will require using multidimensional NMR, but there are several properties of the intact protein that make this approach difficult. Because tropoelastin is enriched in a limited number of hydrophobic amino acids (G, P, L, A, V), severe degeneracy of the NMR signal may arise. A second concern is the size of the protein: even state-of-the-art NMR techniques do not allow an easy structural

† This work was partially supported by the EC "Quality of Life and Management of Living Resources" Program (Contract QLK6-CT-2001-00332), and by MIUR Grant COFIN2002 "Bioactive Synthetic Peptides: Structure, Biological Activity and Innovative Synthetic Procedures".

* Corresponding author: Antonio M. Tamburro, tel. ++39 0971 1011242; fax: ++39 0971 202223; e-mail: tamburro@unibas.it.

[1] Abbreviations: PPII, poly-L-proline II left-handed helix; CD, circular dichroism; NMR, nuclear magnetic resonance; Fmoc, fluorenylmethoxy-carbonyl; DCC, dicloesyl carbodiimide; DSS, 3-(trimethylsilyl)1-propanesulfonic acid; HOBT, hydroxybenzotriazole; TFA, trifluoroacetic acid; MALDI-TOF, matrix assisted laser desorption ionization-time-of-flight; TFE, 2,2,2-trifluoroethanol; TOCSY, total correlation spectroscopy; ROESY, rotating frame NOE spectroscopy; NOE, nuclear Overhauser enhancement, PG II, polyglycine II left-handed helix.

10.1021/bi034837t CCC: $25.00
Published on Web 00/00/0000 PAGE EST: 15.9

determination for a protein containing approximately 750 amino acid residues.

An answer to these technical problems was suggested by the unique organization of the tropoelastin gene (*24*). In all species, the elastin gene exhibits a cassette-like organization with distinct exons encoding for functionally and structurally distinct domains. The basic motif structure is a repeating unit of cross-linking domains followed by domains encoding polypeptide regions putatively responsible for the elastic properties of the protein (*25*).

Studying structural motifs based on individual exons can be useful for elastin (and most probably for other elastomeric proteins) because each exon encodes an independent and self-contained structure. This strategy (the *reductionist* approach) will not apply to other proteins (e.g., globular proteins) where individual exons do not encode autonomously folded structural modules. Furthermore, elastin has been demonstrated to be a fractal protein (*26*), which means that the protein is characterized by the property of statistical self-similarity. Accordingly, even very short sequences show molecular and supramolecular features very similar to those of the whole protein (*27*−*29*). This finding is most likely related to the abundance of repeating sequences of elastin, the repetition being found at different scales along the entire sequence of the molecule (*30*, *27*). Previous results showed that other biological properties of the molecule, such as chemotaxis (*31*−*33*), vasodilatatory activity (*34*), and upregulation of metalloproteinase expression (*35*) are also confined to the sequences coded by particular exons. Accordingly, one can reasonably suggest that studies of isolated domains corresponding to the exons of tropoelastin should give useful insights into both the mechanical as well as biological properties of the protein. Of course, some inherent limitations of this approach are present; for instance, possible interactions between hydrophobic regions cannot be revealed. However, we are confident that this type of reductionist approach to the structure−activity problem of elastin based upon functional units may provide insight into the biologically relevant features of its structure and may lead to the discovery of new biological activities.

In this report, we describe the exon-by-exon synthesis of all polypeptide sequences of human tropoelastin except those pertaining to the polyalanine KA cross-linking domains. The KA domains containing poly-alanine tracts separating two or three lysines have been shown (*36*) to assume an α-helical conformation stereochemically required for the correct juxtaposition of the lysine side chains for desmosine and isodesmosine cross-link formation. Accordingly, only one of these domains, the exon 19 coded peptide, was studied as model of the KA cross-linking domains. CD and NMR data for the synthesized sequences are reported, with detailed structural information for the domains selected to be the most representative.

MATERIALS AND METHODS

Peptide Synthesis and Purification. The peptides were synthesized by using an automatic synthesizer APPLIED BIOSYSTEM model 431 A. Fmoc/DCC/HOBT chemistry was used. The Fmoc-amminoacids were purchased from Nova Biochem (Laufelfingen, Switzerland) and from Inbios (Pozzuoli, Italy). The cleavage of peptide from resin was achieved by using an aqueous mixture of 95% trifluoroacetic acid. 1,2-Ethanedithiol (EDT), phenol, and thioanisol were also used in the cleavage mixture when necessary. The peptides were lyophilized and purified by semipreparative and preparative reversed-phase high-performance liquid chromatography. Binary gradient was used and the solvents were H_2O (0.1% TFA) and CH_3CN (0.1% TFA). The purity of peptides was assessed by either electrospray or MALDI-TOF mass spectrometry.

Circular Dichroism Spectroscopy. CD spectra of 0.1 mg/mL solutions of peptides were recorded on a JASCO J600 CD spectropolarimeter using a HAAKE waterbath as temperature controller using a cell with a 1-mm optical path length. Usually, 16 scans were acquired in the range 190−250 nm at a temperature of 0, 25, or 70 °C by taking points every 0.1 nm, with a 20 nm min^{-1} scan rate, an integration time of 2 s, and a 1 nm bandwidth.

Nuclear Magnetic Resonance Spectroscopy. All ^{1}H NMR experiments were performed on a Varian Unity INOVA 500 MHz spectrometer equipped with a 5-mm triple-resonance probe and z-axial gradients. The purified peptides were dissolved in 700 μL of H_2O/D_2O (90/10) or TFE-d_3/H_2O (70/30), containing 0.1 mM of 3-(trimethyl-sily1)-1-propane sulfonic acid (DSS) as internal reference standard at 0 ppm. Usually 1−3 mM peptide solutions were used. All spectra were collected at 25 °C, unless otherwise stated. One-dimensional ^{1}H spectra were acquired with 32K datapoints and a sweep width of 6000 Hz. TOCSY (*37*) spectra were collected using 256 t1 increments and a spectral width of 6000 Hz in both dimensions. Relaxation delays were set to 2.5 s and spinlock (MLEV-17) mixing time was 80 ms. Shifted sine bell squared weighting and zero filling to 2K × 2K was applied before Fourier transformation. ROESY (*38*) and NOESY data were collected essentially in the same manner as for TOCSY data, with mixing times ranging from 150 to 250 ms. The residual HDO signal was suppressed by presaturation for TOCSY; WATERGATE was used for ROESY and NOESY experiments (*39*). Amide proton temperature coefficients were usually measured from 1D ^{1}H NMR spectra recorded in 5 °C increments from 20 to 45 °C, with the exception of EX26 peptide, for which a series of TOCSY were recorded to measure the amide temperature coefficients. Spectra were processed and analyzed by vnmr Ver. 6.1C software (Varian, Palo Alto, CA).

Resonance Assignments of Elastin Peptides. The EX3, EX4, EX5, EX9, EX11, EX13**,** and EX19 peptides were analyzed by ^{1}H NMR spectroscopy in water (H_2O/D_2O 90/10) and mixed aqueous/organic solution (TFE-d_3/H_2O 70/30) at 25 °C, while EX26 peptide was analyzed only in the latter solution. The resonance assignment of the ^{1}H NMR spectra was made by standard sequential assignment procedures (*40*) and accomplished by a combined analysis of 2D-TOCSY, 2D-ROESY, and 2D-NOESY spectra. TOCSY spectra were used to identify spin systems, while ROESY and NOESY spectra permitted the assignment of resonance to individual amino acids through sequential NOE connectivities.

The presence of unique amino acid residues in several peptides (A2, V13 in EX4; Y8, A16 in EX9; V2, F6, I9, P10 in EX11; K11 in EX13; S4, P5, E6, Y18 in EX19; R1, I10, and F40 in EX26) helped for the resonance assignments, as their resonances were used as starting points in sequential NOE connectivity search.

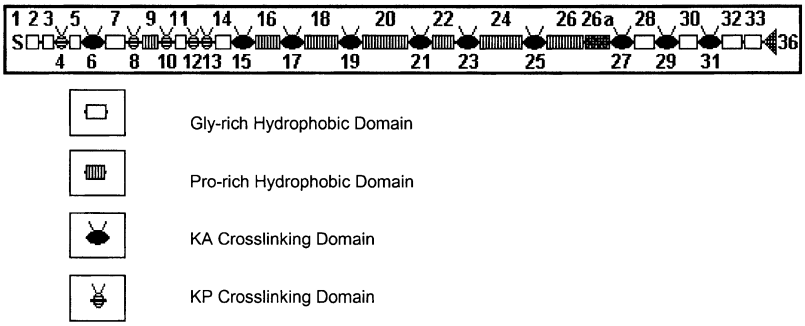

FIGURE 1: Schematic representation of human tropoelastin gene organization. The squares indicate hydrophobic domains, while the circles indicate KP domains. The KA domains are represented by ellipses. The first exon codes for the signal peptide, S, while the last exon 36 codes for a hydrophilic peptide (triangle).

EX2	GVPGAIPGGVPGGVFYP
EX3	GAGLGALGG
EX4	GALGPGG**KP**L**K**PV
EX5	PGGLAGAGLGA
EX7	GAGLGGVPGVGGLGVSA
EX8	GAVVPQPGAGV**KP**G**K**VP
EX9	GVGLPGVYPGGVLPGA
EX10	RFPGVGVLPGVPTGAGV**KPK**AP
EX11	GVGGAFAGIP
EX12	GVGPFGGPQPGVPLGYPI**KA****PK**LP
EX13	GGYGLPYTTG**KL****P**Y
EX14	GYGPGGVAGAAGKAGYPTGT
EX16	GAGAAGVLPGVGGAGVPGVPGAIPGIGGIA
EX18	GAAAGLVPGGPGFGPGVVGVPGAGVPGVGVPGAGIPVVPGAGIPGAAVP
EX19	*GVVSPE**AAAK**AAAK**AAK**Y*
EX20	GARPGVGVGGIPTYGVGAGGFPGFGVGVGGIPGVAGVPSVGGVPGVGGVPGVGIS
EX22	GAAGAGVLGGLVPGPQAAVPGVPGTGGVP
EX24	GLVPGVGVAPGVGVAPGVGVAPGVGLAPGVGVAPGVGVAPGVGVAPGI
EX26	RAAAGLGAGIPGLGVGVGVPGLGVGAGVPGLGVGAGVPGFGA
EX28	GAAVPGVLGGLGALGGVGIPGGVV
EX30	GLVGAAGLGGLGVGGLGVPGVGGLG
EX32	GAAGLGGVLGGAGQFPLG
EX33	GVAARPGFGLSPIFP
EX36	GGACLGKACGRKRK

FIGURE 2: The amino acid sequences of the exon-coded peptides synthesized and analyzed. The underlined sequences are KP cross-linking domains, where the K and P amino acids are in bold. The sequence in italics is the EX19-coded domain, pertaining to the KA cross-linking domains.

For EX4, EX9, EX11, EX13, EX19, and EX26 peptides, the presence of proline in the sequence interrupts the $d_{\alpha N}(i, i+1)$ NOE pathway. In this case, the sequential $d_{\alpha\delta}$(Pro-1, Pro) NOEs for trans conformation or $d_{\alpha\alpha}$(Pro-1, Pro) NOEs for cis conformations were used to identify the resonances of the proline residues. In case of proline containing peptides, cis/trans isomerization can occur, as the energy barrier between the cis ($\omega = 0°$) and trans ($\omega = 180°$) isomers is usually 13−21 kcal/mol (*41*, *42*); nevertheless, we identified in all the peptides one major conformation (>90%) with all trans proline conformers. Thus, the conformational analysis has been carried out only for the major all-trans peptide molecules.

RESULTS

Figure 1 is a schematic representation of the domain structure of human tropoelastin demonstrating the cassette-like organization of the gene, where the exons code alternatively for hydrophobic and cross-linking domains. The hydrophobic domains are responsible for the elasticity of the protein and are rich in glycine, particularly in the N-terminal and C-terminal regions of the protein, and in proline, predominantly in the larger exons localized in the central part of the molecule. The cross-linking domains, alternating with the hydrophobic domains, consist of those rich in alanine (KA domains, central, and C-terminal region), and those containing proline (KP domains, confined principally to first third of the molecule). Three other regions of the protein have unique compositions and functions: exon 1, which encodes a 26-amino acid signal peptide for extracellular transportation; exon 26A, a hydrophilic exon that is a rarely expressed whose function is unknown, and exon 36, which encodes a sequence responsible for interaction with other elastic fiber proteins (*43*).

All of elastin's hydrophobic domains, the KP domains and one example of KA domain (EX19) were synthesized and analyzed. The sequences are presented in Figure 2. CD spectra were recorded at 0, 25, and 60−70 °C to get conformational trends toward the most ordered structures (0 °C) and the most unordered ones (60−70 °C). A brief

Table 1: Secondary Structure Information Determined for the Hydrophobic Domain Peptides by CD Spectroscopy in H_2O and in TFE at Different Temperatures

pept		H_2O	TFE	pept		H_2O	TFE
EX2	0 °C	U + PII[a]	B2 + U + B1	EX20	0 °C	U + PPII	U + B2
	25 °C	U + PII	B2 + U + B1		25 °C	U + PPII	U + B2
	70 °C	U			70 °C	U + PPII	U + B2
EX3	0 °C	PPII	B2 + U	EX22	0 °C	U	B2 + U
	25 °C	PPII + U	B2 + U		25 °C	U	B2 + U
	70 °C	U	U		70 °C	U	B2 + U
EX5	0 °C	PPII	U + B1/B2	EX24	0 °C	U + PPII	U + B2
	25 °C	PPII + U	U + B1/B2		25 °C	U + PPII	U + B2
	70 °C	U	U + B1/B2		70 °C	U	
EX7	0 °C	U	U + B2	EX26	0 °C	U + PPII	U + B2
	25 °C	U	U + B2		25 °C	U	U + B2
EX9	0 °C	U + PPII	B1 + B2 + U	EX28	0 °C	U + PPII	B1 + U
	25 °C	U + PPII	B1+B2+U		25 °C	U + PPII	B1 + U
EX11	0 °C	U + ARc	ARc	EX30	0 °C	PPII	B2 + U
	25 °C	U + ARc	ARc		25 °C	BS + PPII	B2 + U
	70 °C	U + ARc			70 °C	U	
EX14	0 °C	ARc + U	B2 + U	EX32	0 °C	PPII	B1/B2 + U
	25 °C	ARc + U	B2 + U		25 °C	PPII + U	B1/B2 + U
	70 °C		B2 + U		70 °C	U	B1/B2 + U
EX16	0 °C	PPII+U	B2 + U	EX33	0 °C	PPII	U + B1/B2
	25 °C	U	B2 + U		25 °C	U	U + B1/B2
	70 °C	U	B2 + U		70 °C	U	U + B1/B2
EX18	0 °C	U + PPII	U + B2	EX36[b] r	25 °C	U	B1 + U
	25 °C	U + PPII	U + B2	EX36 o	25 °C	U + B1	U + B1

[a] U, unordered; B1, type I β-turn; B2, type II β-turn; PPII, poly-proline II helix; BS, β-strand; ARc, aromatic contributions. [b] r, cysteine in reduced form; o, with intramolecular disulfide bridge

overview will be presented below. We also provide a detailed CD and NMR analysis of the most representative sequences: exon 3 (EX3), exon 5 (EX5), and exon 11 (EX11)-as models of glycine-rich hydrophobic domains; exon 9 (EX9) and exon 26 (EX26) as representative of proline-rich hydrophobic domains; and exon 4 (EX4) and exon 13 **(**EX13**)** as models of KP cross-linking domains, and exon 19 (EX19) as example of KA cross-linking domains.

Secondary Structure Analysis. The microenvironment that determines the conformation of an amino acid sequence is not known a priori and can be different from the bulk macroscopic solution conditions (i.e., physiological conditions). Predicting the functional solvent environment for insoluble elastin is particularly difficult because the protein's hydrophobicity and highly cross-linked nature suggest a less polar internal environment than the surrounding solvent. For this reason, the experiments in this study were performed in both water and 2,2,2-trifluoroethanol (TFE). TFE is a significantly less polar solvent than water and is usually considered a structure-inducing solvent because it favors intramolecular hydrogen bonding, thus promoting folded conformations such as helices and β-turns (*44*−*46*). While the real local solution conditions for insoluble elastin are unknown, it is likely to be intermediate between the two solvent extremes of water and TFE.

Tables 1 and 2 contain a summary of the CD data for all 24 sequences that were analyzed. To detect temperature-induced conformational transitions, the peptides were monitored by CD spectroscopy at different temperatures. For some peptides, isoelliptic points were evident, indicative of the presence of an equilibrium between two conformations with one being more stable at low temperature and the other, usually the unordered conformation, more prevalent at higher temperature. In particular, isoelliptic points were observed for EX2, EX5, EX10, EX14, EX24, EX26, and EX30 peptides in water, where conformational equilibria between PPII and unordered conformations are proposed. The same was observed for EX19 peptide where an equilibrium between α-helix and unordered conformation was found in TFE.

CD deconvolution programs were not useful in establishing realistic values for the conformation of elastin peptides. Table 3, for example, shows the results of EX5 peptide CD curve analysis at 0, 25, and 70 °C in water analyzed using the CDPro software package (available at http://lamar.colostate.edu/∼sreeram/CDPro/main.html) (*47*). This program package provides three different deconvolution methods: Selcon, the self-consistent method (*48*); ContinLL, a variant of the CONTIN method (*49*); and CDsstr, a method developed by Johnson (*50*) using the single value decomposition algorithm. The reference databases consist predominately of CD spectra of globular proteins of known secondary structure.

What emerged from the CDPro analysis of our peptides was that the CD spectra of elastin peptides are not well represented in the reference proteins, so these programs are not suited for CD analysis of the hydrophobic and flexible peptides present in elastin sequence. For this reason, CD spectra of the different sequences were analyzed by comparing the curves with CD spectra of peptides with known secondary structures or with peptides that adopt a mixture of known structures (*51*).

Several general conclusions can be made from the complete CD analysis of the sequences: (i) in water, the elastin sequences show a predilection for the flexible PPII conformation; (ii) in less polar conditions, folded conformations, especially type I and type II β-turns, are present. These conformations are quite stable as an increase of temperature produces only minor changes in the CD spectra. (iii) Peptides with aromatic residues give poor secondary structure information when the degree of freedom of the aromatic residue is reduced by the folded conformation. (iv) The conformations adopted by KP cross-linking domains are similar to hydrophobic domains, with a preference for PPII in water and folded conformations in TFE. (v) The KA cross-linking domain has a great propensity to adopt α-helical structure that increases in TFE solution.

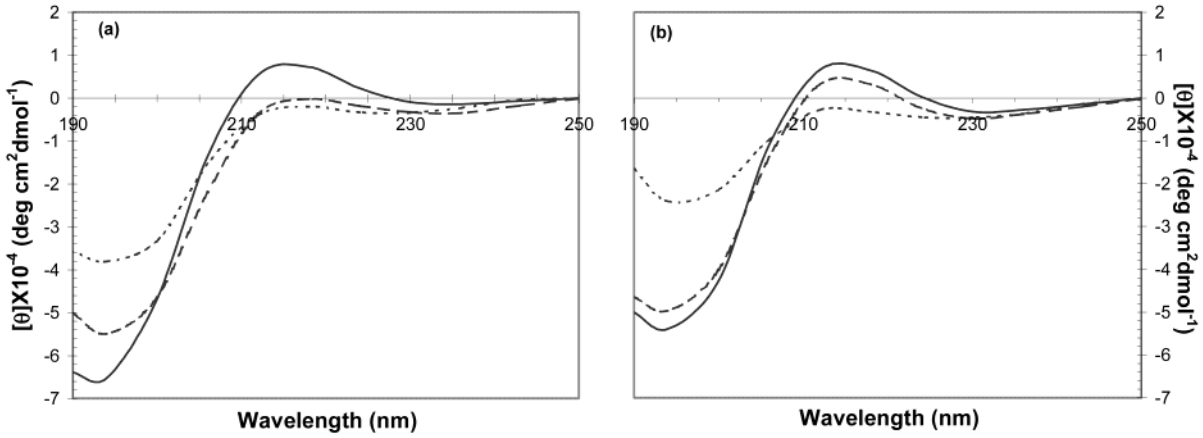

FIGURE 3: CD spectra of EX3 peptide in water (a) and in TFE (b) recorded at different temperatures: (—) at 0 °C, (—— —— —) at 25 °C, (- - -) at 70 °C.

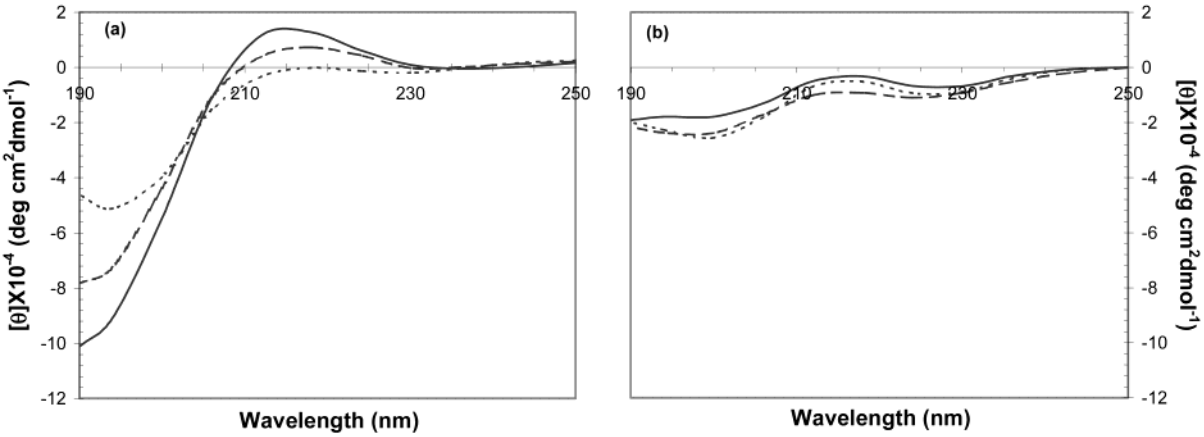

FIGURE 4: CD spectra of EX5 peptide in water (a) and in TFE (b) recorded at different temperatures: (—) at 0 °C, (—— —— —) at 25 °C, (- - -) at 70 °C.

Table 2: Secondary Structure Information Determined for the KP Cross-Linking Domain Peptides and the KA Cross-Linking Domain Peptide (EX19) by CD Spectroscopy in H_2O and in TFE at Different Temperatures

peptide		H_2O	TFE
EX4	0 °C	U[a]	B1 + U
	25 °C	U	B1 + U
	70 °C	U	
EX8	0 °C	U + PPII	B1/B2 + U
	25 °C	U + PPII	B1/B2 + U
	70 °C	U + PPII	B1/B2 + U
EX10	0 °C	U + PPII	B1 + U
	25 °C	U + PPII	B1 + U
	70 °C	U + PPII	B1 + U
EX12	0 °C	U + PPII	B1/B2 + U
	25 °C	U + PPII	B1/B2 + U
	70 °C	U + PPII	B1/B2 + U
EX13	0 °C	ARc	B1/B2 + U +ARc
	25 °C	ARc	B1/B2 + U +ARc
EX19	0 °C	H + U	H
	25 °C	H + U	H + U
	70 °C	U + H	H + U

[a] U, unordered, B1, type I β-turn, B2, type II β-turn, PPII, poly-Proline II helix, ARc, aromatic contributions, H, α-helix.

Table 3: CDPro Deconvolution Results for EX5 Peptide CD Spectra in Water at Different Temperatures

	α-helix	β-sheet	turn	PPII	Unrd	RMSD
			SELCON			
0 °C	0.006[a]	0.183	0.068	0.055	0.755	0.449
25 °C	0.122	0.561	0.117	0.038	0.243	0.181
70 °C				no solutions		
			ContinLL			
0 °C	0.041	0.286	0.116	0.124	0.433	0.115
25 °C	0.042	0.276	0.127	0.112	0.443	0.072
70 °C	0.010	0.277	0.111	0.121	0.481	0.060
			CDsstr			
0 °C	0	0.301	0.136	0.115	0.439	0.204
25 °C	0	0.305	0.136	0.117	0.428	0.139
70 °C				no solutions		

[a] Fraction of secondary structure in the molecule.

To assess whether the elastin peptides have a preferred backbone conformation under the different solution conditions, detailed CD and NMR analysis of peptides EX3, EX4, EX5, EX9, EX11, EX13, EX19, and EX26 were conducted.

Glycine-Rich Hydrophobic Domains: EX3, EX5, and EX11. Peptides EX3, EX5**,** and EX11 have sequences particularly rich in glycine residues (5 out of 9 residues for EX3, 5 out of 11 residues for EX5, and 4 out of 10 residues for EX11) and are expected to exhibit a high degree of chain flexibility with no particular tendency to form regular secondary structures such as helices, β-sheets, or β-turns. EX3 peptide contains only three types of amino acid residues, alanine, glycine, and leucine, while EX5 peptide includes an N-terminal proline residue. EX11 peptide contains the β-branched amino acids valine (V2) and isoleucine (I9), together with an aromatic residue (F6).

The CD spectra, recorded in water (Figure 3a and Figure 4a), for EX3 and EX5 peptides at 0 °C show a strong negative band around 194 nm and a weak positive band at

~216 nm. As the temperature is increased from 0 to 70 °C, the strong negative band is slightly red-shifted and reduced in intensity, while the positive band disappears. Furthermore, for EX5 peptide an isoelliptic point is evident, suggesting the presence of only two conformations in solution.

The strongly negative $\pi-\pi^*$ band at ~194 nm is usually attributed either to unordered or PPII conformations, but its reduction in intensity with increasing temperature, a property typical of the PPII conformation (*52*) leads us to attribute it to the latter conformation. The positive, essentially $\pi-\pi^*$ band at ~216 nm is another typical feature of PPII structure (*53*−*56*). Together, these properties of the spectra at 0 °C represent, with good approximation, a classical PPII spectrum of peptides lacking proline. For peptides rich in proline or hydroxy-proline, the positive band is shifted to ~225 nm due to the presence of tertiary amide chromophores (*57*).

The presence of a high content of PPII conformation in these peptides (EX3 and EX5) is not surprising when the amino acid composition and properties of the basic sequences are considered: (i) the high glycine content of the peptides and the intrinsic propensity of glycine residues to adopt a PPII conformation, as poly-glycine can adopt the PGII left-handed 3_1 helix structure (*58*) similar to PPII as characterized in the solid state by X-ray diffraction (*59*); (ii) the relative high intrinsic propensity of alanine, glycine, and leucine to adopt a PPII conformation, as pointed out by host−guest studies (*60*) and by Molecular Dynamics simulations (*61*, *62*); (iii) the presence of -LG- units in the sequences. This dipeptide has a tendency to adopt PPII conformation as determined by X-ray diffraction studies (*63*).

The NMR analysis of EX3 (Figure 5 A) and EX5 (Figure 5C) peptides in aqueous solution were characterized by the absence of medium or long range NOEs of the backbone protons. This finding clearly indicates the absence of any helix or β-sheet structure. Chemical shift index (CSI) analysis (the analysis of the deviation of Hα chemical shift from random coil values) (*64*) confirms these structural predictions as all the Hα chemical shifts are inside the random coil range. Furthermore, the temperature coefficients of EX3 and EX5 peptide amide resonances are high ($>5.2 \times 10^{-3}$ ppm K^{-1}), suggesting that the backbone amide groups are not involved in either intramolecular or intermolecular H-bonding, but are exposed to the solvent.

Analysis of the $^3J_{NH-H\alpha}$ coupling constants, related to the torsion angle ϕ by the Karplus equation (*65*), indicated that the presence of extended β-strand conformation can be excluded, as the values are ~6−7 Hz, below the 9 Hz value typical of β-strand conformation. However, the interpretation of coupling constants in terms of specific conformations should always be done cautiously, especially when there is extensive conformational averaging. This is because the coupling constants are the least sensitive parameters for structure detection (*66*).

In our case, for instance a value of 6.5 Hz could be due either to an unordered conformation that populates different ϕ angle conformations, or to a single conformation with a ϕ angle value of −78 as related by Karplus equation.

Nevertheless, by excluding β-strand and α-helix conformations, only two possibilities need to be considered for the EX3 and EX5 peptides structures in water: unordered structure or PPII conformation as suggested by CD spectroscopy. To distinguish between these two possibilities by NMR, however, is not straightforward, as the PPII structure has no unique NMR signature that allows unambiguous structure determination (*55*). Furthermore, the presence of both conformations in equilibrium cannot be excluded. There are indications, however, that distinguish between a totally random conformation and a quasi-extended left-handed PPII helix. The most important property of PPII conformation is the absence of either sequential or long-range d_{NN} NOE, because the distance of two sequential amide protons in a regular PPII helix is greater than 4.6 Å. As a result, the intensity ratio between sequential $d_{\alpha N}(i,i+1)$ and $d_{NN}(i, i+1)$ NOEs is very high, as expected for an extended conformation

A)

EX3[a]	G1	A2	G3	L4	G5	A6	L7	G8	G9
dαN(i,i+1)									
dαN(i,i)									
dNN(i,i+1)									
$^3J_{NH\alpha}$[c]	-	6.0	12.0	#[d]	12.0	6.1	#	12.0	11.7
Δδ/ΔT	-	-6	-6.8	#	-6	-6.4	#	-6.9	-5.9

B)

EX3[b]	G1	A2	G3	L4	G5	A6	L7	G8	G9
dαN(i,i+1)									
dαN(i,i)									
dNN(i,i+1)									
dαN(i,i+2)									
$^3J_{NH\alpha}$[c]	-	8.7	12.0	7.0	11.9	7.8	8.5	12.2	12.0
Δδ/ΔT	-	-5.0	-5.3	-5.0	-5.6	-5.7	-4.1	-3.9	-4.2

C)

EX 5 [a]	P1	G2	G3	L4	A5	G6	A7	G8	L9	G10	A11
dαN(i,i+1)											
dαN(i,i)											
dNN(i,i+1)											
$^3J_{NH\alpha}$[c]	-	11.8	#	6.9	#	11.8	6.5	#	7.3	12.5	6.8
Δδ/ΔT	-	-5.8	#	-6.8	-6.0	-6.2	-5.4	#	-6.6	-6.6	-5.8

D)

EX 5 [b]	P1	G2	G3	L4	A5	G6	A7	G8	L9	G10	A11
dαN(i,i+1)											
dαN(i,i)											
dNN(i,i+1)											
dαN(i,i+2)											
$^3J_{NH\alpha}$[c]	-	11.7	11.6	6.8	5.8	11.4	6.1	12.1	7.0	12	7.0
Δδ/ΔT	-	-4.8	-5.6	-5.9	-5.3	-3.7	-3.4	-5.0	-4.0	-4.8	-4.2

[a] spectra recorded in H_2O/D_2O 90/10 at 298K

[b] spectra recorded in TFE-d_3/H_2O 70/30 at 298K

[c] The ^3J values for Gly residues are the sum of J_{AX} and J_{BX}, [d] # (not determined)

FIGURE 5: Summary of NMR parameters of EX3 peptide: (A) in water and (B) TFE-d_3/H_2O 70/30; EX5 peptide: (C) in water and (D) in TFE-d_3/H_2O 70/30. The summary includes sequential and medium range NOEs, the ^3J coupling constants (Hz), and temperature coefficients ($\Delta\delta/\Delta T$, ppb/K). The NOE intensities are reflected by the thickness of the lines. When an unambiguous assignment was not possible due to peak overlap, the NOEs are drawn with gray lines.

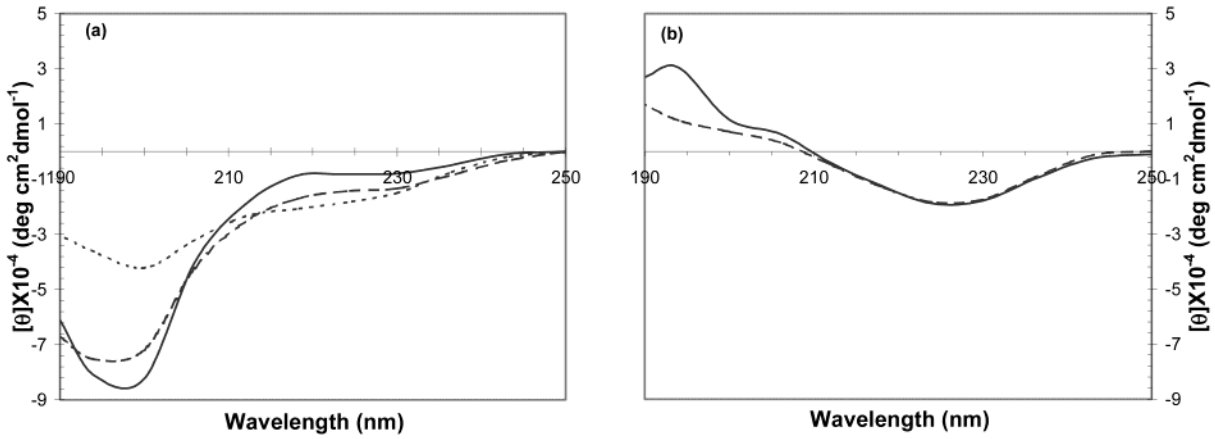

FIGURE 6: CD spectra of EX11 peptide in water (a) and in TFE (b) recorded at different temperatures: (—) at 0 °C, (— — —) at 25 °C, (- - -) at 70 °C.

(*67*), which is distinctly different from the same ratio in the case of random structures. Using a population weighted random coil model, the intensity ratio between these two NOEs was predicted to be 1.4 (*68*), very different from the PPII conformation where it is evaluated as ∼55. Analyzing EX3 peptide in water we noted the absence of $d_{NN}(i, i+1)$ NOEs for the sequences G2−L4 and A6−G8 whereas the d_{NN} sequential NOEs (L4−G5, G5−A6, G8−G9) were of reduced intensity (Figure 5A). This suggests that the residues of the peptide mostly populate the upper left region of the Ramachandran map where PPII is located. Also, for EX5 peptide, the reduced intensity of the $d_{NN}(i,i+1)$ NOEs points to the presence of significant PPII conformation in water (Figure 5C). Together with the CD spectra, all of the NMR data confirm the presence of PPII helix in water for the peptides EX3 and EX5.

In contrast to peptides EX3 and EX5, the CD spectra of EX11 suggest little PPII structure in water, where a negative band at 195 nm and the absence of the positive band at 216 nm indicate a predominant unordered conformation (Figure 6a). It is likely that the presence of β-branched amino acids in this peptide destabilizes the PPII conformation by decreasing the stabilizing solvation effect of water (*60*, *69*). The absence of any preferred conformation was confirmed by NMR data (NOE, coupling constants), although a very low temperature coefficient for residue G8 could suggest the presence of one H-bond (Figure 7A). As no typical NOEs for folded conformations have been found, however, the unusually low-temperature coefficient has to be attributed to the interaction of the aromatic ring of F6 with the peptide's backbone. This would reduce the exposure of the NH amide proton of G8 to the solvent, as suggested by studies with other peptides (*70*).

In the hydrogen bond promoting solvent TFE, the CD spectra of EX3 peptide are similar to spectra obtained with aqueous solution at different temperatures (Figure 3b). In particular, a positive band at 216 nm is still evident at 25 °C. This behavior is unusual because the PPII content is typically higher in water than in organic solvents because the water molecules stabilize this structure by a hydrogen-bonded network involving the backbone polypeptide (*71*, *61*) This raises the possibility that the positive band at ∼216 nm is due to the presence of type II β-turn together with unordered conformation rather than to PPII structures alone. Indeed, NMR analysis of the EX3 peptide in the less polar solvent mixture (TFE-d_3/H_2O 70/30) showed evidence for a type II β-turn between G5 and G8 (Figure 5B). A reduced temperature coefficient for the G8 amide proton (−3.9 ppb/K) and typical β-turn NOEs are also evident. Supporting the β-turn structure is the presence of medium range NOE $d_{\alpha N}$-(i,i+2), which is the most striking indication of the presence of a reverse turn conformation. The absence of d_{NN} NOE, together with a strong $d_{\alpha N}$ sequential NOE between residue i+1 and i+2 of the turn further established the presence of a type II β-turn.

EX5 peptide has a sequence similar to EX3, containing a common hexapeptide unit GAGLGA. Its behavior in TFE, however, is different, as no positive band at 216 nm is evident (Figure 4b). At 0 °C, the CD spectrum is attributed to a mixture of unordered and type I β turn conformations, while at 25 and 70 °C the content of β-turn is significantly decreased.

Strong aromatic contributions dominate the CD spectra of EX11 (Figure 6b) in TFE. These side chain contributions, more evident at 0 °C than at 25 °C, suggest a reduced conformational freedom of the aromatic ring most likely the consequence of a folded conformation (*72*, *73*).

NMR data confirmed the presence of a β-turn spanning the sequence A5−G8, thus positioning the F6 at the corner of the β-turn (Figure 7B).

Proline-Rich Hydrophobic Domains: EX9 and EX26. EX9 and EX26 peptides contain three and four proline residues, respectively, positioned uniformly throughout a sequence of 16 and 42 residues and serve as a model for the proline rich domains of elastin. Even though the EX9 peptide contains both types of beta turn promoting sequences (-PG- and -GG-), CD analysis of the peptide in water showed the presence of PPII conformation. As shown in Figure 8a, at 0 °C a strong negative $\pi-\pi^*$ band is evident around 200 nm together with a small positive band at longer wavelengths. With increasing temperature, the ellipticity at short wavelengths becomes less negative, while at longer wavelengths it becomes more negative. This behavior is usually attributed to a conformational equilibrium between PPII and other conformations (*52*). The absence of isoelliptic points in the spectra suggest the presence of complex equilibria with more than two conformations, probably a mixture of PPII, unordered and β-turn conformations. The NMR data were not able to resolve the presence of preferred conformations for this peptide in water, thus suggesting very flexible structures (Figure 7C).

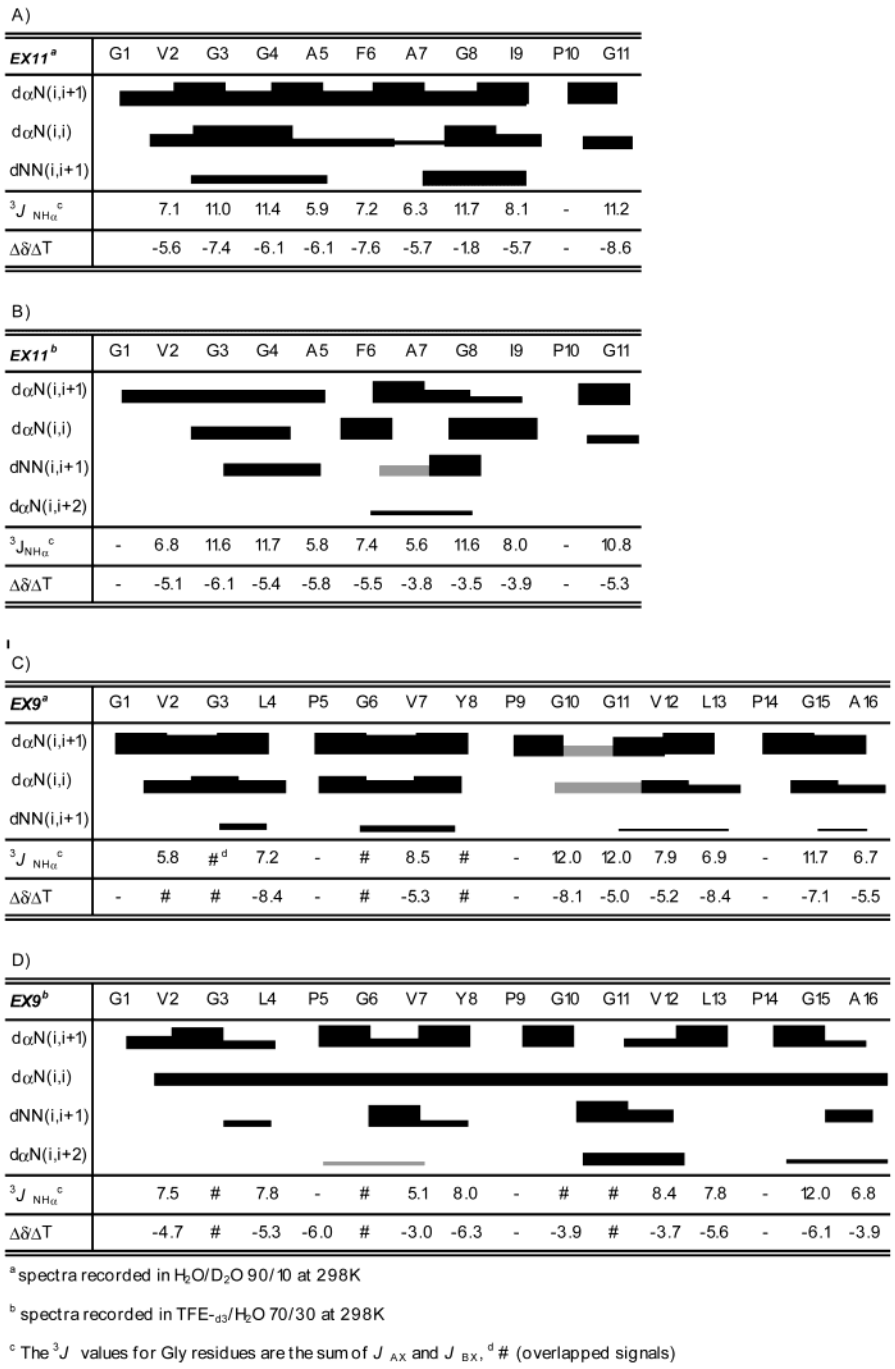

FIGURE 7: Summary of NMR parameters of EX11 peptide: (A) in water and (B) in TFE-d_3/H_2O 70/30; EX9 peptide: (C) in water and (D) in TFE-d_3/H_2O 70/30. The summary includes sequential and medium range NOEs, the ^3J coupling constants (Hz), and temperature coefficients ($\Delta\delta/\Delta T$, ppb/K). The NOE intensities are reflected by the thickness of the lines. When an unambiguous assignment was not possible due to peak overlap, the NOEs are drawn with gray lines.

The CD spectra of EX9 in TFE, as shown in Figure 8b, showed the presence of a positive band at ~205 nm and a negative band at ~220 nm that is slightly red-shifted and reduced in intensity with increasing temperature. The curve at 0 °C resembles the CD spectra described by Perczel et al. containing contributions from 60% type II β-turn, 20% type I β-turn, and 20% unordered conformations (*51*).

The positive band at 205 nm is probably due to type II β-turn, whereas the negative band could be due dominantly to type I β-turn. The intensity of the negative band is reduced with increasing temperature, suggesting a reduced stability of type I β-turn.

NMR analysis of EX9 in TFE-d_3/H_2O (70/30) confirmed the presence of both type I and type II β-turns (Figure 7D). The type II β-turns were located in the regions L4−V7 and L13−A16 and contained in both cases -PG- units at the corners. The type I β-turn, situated in the region P9−V12, had the flexible -GG- sequences at the corners. The occurrence of rather low-temperature coefficients (<4.0 ppb/K) for the amide protons (V7, V12, and A16), usually attributed to hydrogen bonding of the amide proton to the peptide backbone, is one element for the assessment of reverse turns in peptides. In the case of turns, the lowered temperature coefficient is due to the presence of a hydrogen bond between

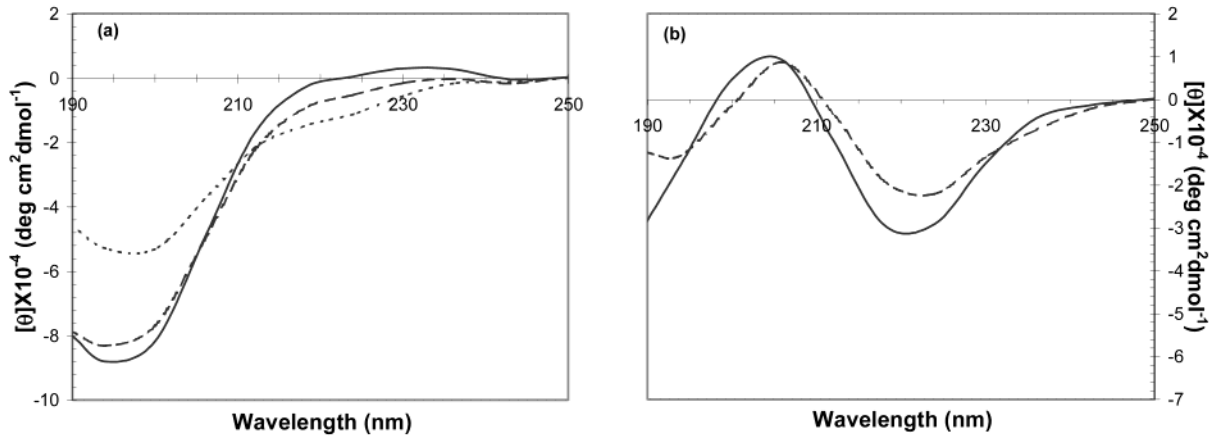

FIGURE 8: CD spectra of EX9 peptide in water (a) and in TFE (b) recorded at different temperatures: (—) at 0 °C, (−− −− −) at 25 °C, (- - -) at 70 °C.

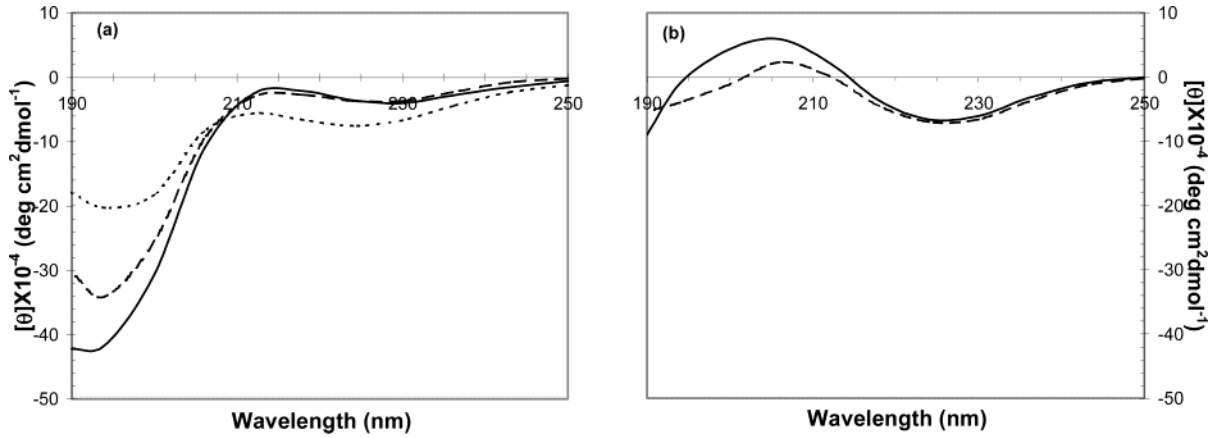

FIGURE 9: CD spectra of EX26 peptide in water (a) and in TFE (b) recorded at different temperatures: (—) at 0 °C, (−− −− −) at 25 °C, (- - -) at 70 °C.

the NH of residue i+3 of the turn with the CO of residue i. One of the most important diagnostic features of a reverse turn conformation is the close approach of Hα of residue i+1 with the NH of residue i+3 of the turn. The NOE effect arising from this interaction is usually weak, because the distance involved is ∼3.4 Å. However, the existence of this typical medium range NOE is a good indication of a significant population of turn conformation present in solution (*70*).

Different NOEs patterns also provide a way to distinguish between different turns, as pointed out previously. Indeed, a type I β-turn shows strong sequential d_{NN} NOEs for residue i+1, i+2 and for residue i+2, i+3 of the turn. A type II β-turn shows a strong sequential NOE $d_{\alpha N}$ (i+1, i+2) of the turn together with an intense d_{NN}(i+2, i+3) NOE. In the case of the EX9 peptide, we can detect the presence of typical medium range NOEs: $d_{\alpha N}$(i, i+2) P5/V7, G10/V12, and P14/A16, together with the usual pattern of sequential NOEs for type I β-turn for the sequence P9−V12, and for type II β-turns for the sequence L4-V7 and L13-A16 (Figure 7D).

Also EX26 peptide comprises four beta turn promoting sequences -PG-: accordingly, the CD spectra of the peptide in TFE indicate at 0 °C the presence of a weak positive band at about 205 nm and a negative one at 226 nm, possibly due to type II β-turn together with open conformations (Figure 9 b). Increasing the temperature induces the reduction of the positive band due to the instability of the turn.

The presence of a repeated unit, $(PGLGVGXGV)_3$ with X = V, A, in the sequence slightly facilitated the NMR studies of the 42-residue-long EX26 peptide in TFE-d_3/H_2O (70/30). Indeed, even if the complete assignment of all the glycine residues was not possible because of severe overlap (Figure 10 B), almost all nonglycine residues were assigned, allowing one to highlight some interesting results. In particular, the TOCSY spectra showed that some residues of the repeated unit have equivalent chemical shifts in the three repeats; as a consequence, it was possible to identify only one type of proline residue for all four prolines, suggesting that all the proline residues have a homogeneous microenvironment; also for the leucine residues only two types were recognized, one of reduced intensity assigned to the L6 and the other assigned to L13, L22, and L31 inside the nonapeptide repeat. A similar behavior was found for the valine residues, where three different types were revealed. On the contrary, for the alanine as well as for the glycine residues very different amide chemical shift were found (Figure 10B). The temperature dependence of not overlapping residues was determined by recording TOCSY spectra at different temperatures. The amide protons of L13, L22, and L31 show a reduced temperature coefficient (3.4 ppb/K), suggesting the involvement of these residues in hydrogen bond formation (Figure 10A). From these data together with typical NOEs we concluded that -PG- moieties also in EX26 peptide favor the formation of β-turns.

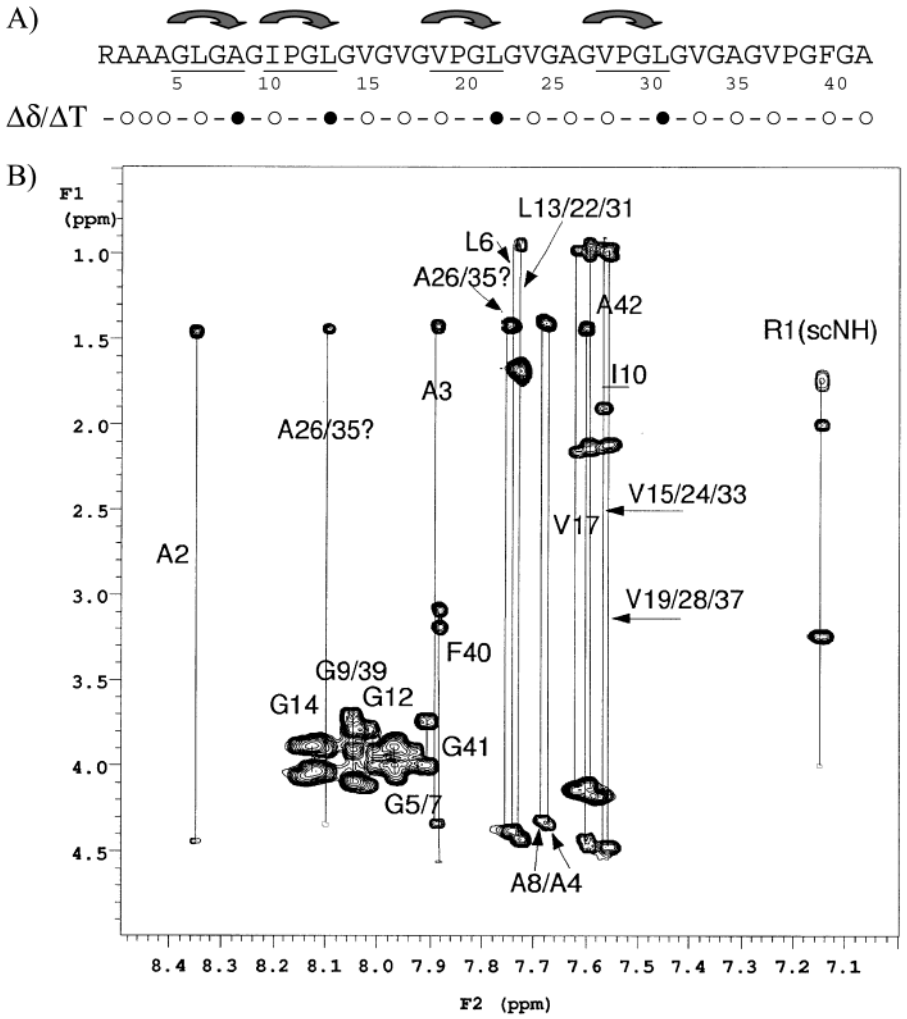

FIGURE 10: (A) In the first row the sequence of EX26 is shown. Proposed turn positions are indicated by arrows; in the second row the temperature coefficients of not overlapping residues are reported (○, >4.0 ppb/K; ●, ≤4.0 ppb/K). (B) A section of the TOCSY spectrum of EX26 in TFE-d_3/H_2O (70/30) at 25 °C, with indication of residue assignments.

The CD spectra of EX26 peptide in water are completely different (Figure 9a). At 0 °C, a strong negative band below 200 nm and a small one at about 228 nm appear. Moreover, a peak at about 215 nm is present, suggesting a trend toward a positive band typical of PPII structure. The rising of the temperature induces a significant decrease of the negative band. This behavior is typical of a random coil in equilibrium with PPII conformation, as strongly suggested by the presence of an isoelliptic point.

KP Cross-Linking Domains: EX4 and EX13. The putative KP cross-linking domains typically contain two lysine residues separated by one or two amino acids, of which one is a proline. The presence of proline hinders the formation of α-helix, which is the typical conformation for the KA cross-linking domains. KP domains most likely do not participate in the formation of the quaternary cross-links desmosine or isodesmosine, but, as suggested by Mecham and co-workers for exon10 (*43*), are thought to contribute lysine side chains to the binary cross-links lysinonorleucine or allysine aldol. For this reason, it is of particular interest to identify the conformation adopted by these domains and to discern the spatial conformation of the lysine side chains. The CD spectra of EX4 in water suggest a fully random coil conformation, which was also confirmed by NMR studies (Figure 12A). The CD spectrum of the peptide in TFE, however, shows a decrease in intensity of the 194 nm negative band, suggesting a reduction in unordered conformation content. An increase in the negative band at 225 nm suggests the presence of type I β-turn (Figure 11b).

NMR studies in TFE-d_3/H_2O (70/30) localized the turn to P5−K8, where a very stable type I β-turn is evident (Figure 12B). It is important to note the very low-temperature coefficient of K8 (-0.3×10^{-3} ppm K^{-1}), indicating a strong hydrogen bond. It was not possible to identify the typical medium range NOE of turns, $d_{\alpha N}(i+1, i+2)$, because of overlap of the signals, but the presence of strong sequential d_{NN} NOEs suggests a high population of turn conformation. Interestingly, only K8 is involved in this folded structure, while the K11 is localized in a highly flexible region. Probably, these different structural conformations suggest a different susceptibility of these two lysines to lysyl oxidase (LOX). This suggestion seems quite reasonable, if we compare the dihedral angles of the type I β-turn, involved often in nascent helix folding (residue i+1: $\phi = -60$, $\psi = -30$; residue i+2: $\phi = -90$, $\psi = 0$), with those of a regular α−helix ($\phi = -57$; $\psi = -47$), the common substrate conformation for LOX in elastin. These findings are compatible with a proposal implying that K8 could be involved in allysine aldol cross-links while K11 contributes to a lysinonorleucine cross-link through its ϵ-ammino group.

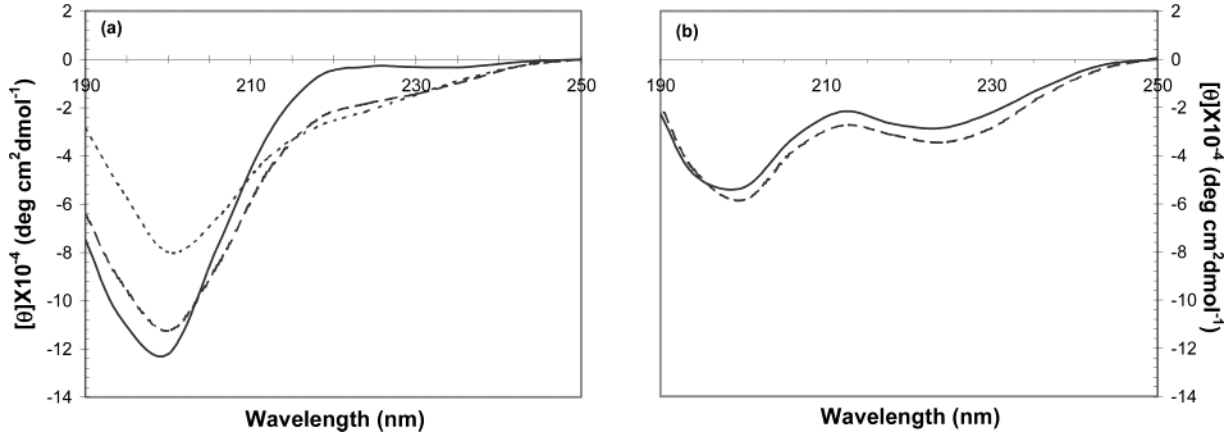

FIGURE 11: CD spectra of EX4 peptide in water (a) and in TFE (b) recorded at different temperatures: (—) at 0 °C, (–– –– ––) at 25 °C, (- - -) at 70 °C.

The exon 13 coded peptide exhibits only one lysine residue in the sequence, but it is considered a KP cross-linking domain through analogy with bovine tropoelastin sequence where two lysines are present. It should, however, be considered an atypical cross-link domain. The CD spectra of peptide EX13 in water as well as in TFE were difficult to interpret (Figure 13). It is likely that the aromatic contributions of the three tyrosines (Y3, Y7, Y14) in the peptide sequence dominate over peptide transitions. The 230 nm band is clearly assigned to tyrosine side chains, but tyrosine is also known to contribute to the 190−200 nm region. These aromatic contributions make it difficult to extrapolate any secondary structure information from CD spectra. Thus, for this peptide, only the NMR data were informative. NMR analysis of EX13 in TFE suggested the presence of a type II β-turn in the region G2−L5, positioning the aromatic residue (Y3) at the corner of the turn, thus clarifying the high aromatic contribution to the CD spectra (Figure 12D). Few indications for folded conformations are present in the region where the lysine is positioned.

KA Cross-Linking Domains: EX19. The exon 19 (EX19) coded peptide corresponds to a sequence highly representative of those domains involved mainly in the formation of desmosine and isodesmosine cross-links. This domain, together with exon 25 (KA domain) and exon 10 (KP domain) coded domains, was suggested to be important for nucleating the assembly process of tropoelastin (*43*). Its sequence comprises three lysine residues, two of which are involved in desmosine/isodesmosine cross-link formation, while the third one is implicated in lysinonorleucine cross-links.

As expected, the CD spectra (Figure 14) recorded in water and TFE are typical of dominantly α-helical structures. Of course, the amount of α-helix is higher in TFE than in water as judged by the higher ellipticities at about 220, 207, and 190 nm.

The NMR studies in TFE-d_3/H_2O 70/30 (Figure 15) showed a very stable secondary structure, constituted by an α-helix spanning the region E6−A15, preceded by a type I β-turn involving S4−A7. The presence of the α-helix is demonstrated by typical short and medium range NOEs (strong δ_{NN} (i,i+1); medium δ_{NN} (i,i+2); strong $\delta_{\alpha\beta}$(i, i+3)), as well as by $^3J_{NH-H\alpha}$ coupling constants of 4.0−4.5 Hz and by chemical shifts of the Hα below the tabulated random coil values (CSI < 0). The presence of the turn is indicated by a very low-temperature coefficient (2.4 ppb/K) of A7 and by the presence of medium range NOEs involving Hβ of V2 and Hα of P5 and Hβ *o*f V3 and Hα of E6, which is possible only in the case of a turning back of the polypeptide chain.

In aqueous solution, some NOEs typical of the α-helix were still present, even though of reduced intensity, suggesting a less stable structure, as confirmed also by $^3J_{NH-H\alpha}$ coupling constants of 5.0−5.5 Hz. Also, the CSI analysis suggests that the helix size is reduced to the region A7−K10. The β-turn in the region SPEA was no longer present as confirmed by the higher temperature coefficient of A7 (4.8 ppb/K) and by the absence of typical NOEs. It is important to note that the presence of significant amounts of α-helix even in aqueous solution can be attributed to a stabilizing electrostatic interaction between E6 and K10 side chains which are positioned in the helix at suitable distance (i, i+4) for salt-bridge formation. In fact, CD and NMR analyses on a synthetic peptide lacking the N-terminal sequence GVVSPE evidenced the loss of α-helical structure in aqueous solution (data not shown).

DISCUSSION

The results described in this paper give precise and detailed information about the most significant structures populating the elastin molecule. On the whole, the conformational features found for the single exon coded polypeptides are the same as those previously suggested for the entire protein, even though they were not yet associated with specific sequences. A key aspect of the elastin molecule that makes an exon-by-exon analysis practical is that each exon encodes an independent and self-contained structure. Confirmation that this approach can be successful is our finding that a synthetic peptide encoding a KA-type cross-linking region (exon 19) is α-helical in aqueous solution, in agreement with experimental findings for a KA-type cross-link containing peptide isolated from the intact elastin molecule (*36*). Thus, the structure of exon 19 does not require flanking sequences from adjacent exons to assume a correct conformation. Indirect evidence that the exonic sequences are structurally correct is the finding that some, such as 18, 20, 24, are able to coacervate (at high concentration and in the presence of NaCl) in a manner similar to the intact tropoelastin molecule. Other peptides, such as that encoded by exon 30, adopt fibrillar supramolecular structures typical of elastin (unpub-

A)

EX4[a]	G1	A2	L3	G4	P5	G6	G7	K8	P9	L10	K11	P12	V13
dαN(i,i+1)													
dαN(i,i)													
dNN(i,i+1)													
$^3J_{NH\alpha}$[c]		5.8	6.4	11.7	-	11.0	12.0	8.0	-	5.0	7.5	-	8.5
Δδ/ΔT		#[d]	#	-6.5	-	-7.0	-4.0	-3.7	-	#	-8.0	-	-8.1

B)

EX4[b]	G1	A2	L3	G4	P5	G6	G7	K8	P9	L10	K11	P12	V13
dαN(i,i+1)													
dαN(i,i)													
dNN(i,i+1)													
dαN(i,i+2)													
$^3J_{NH\alpha}$[c]	-	6.0	8.4	11.2	-	11.8	11.9	7.9	-	7.1	7.7	-	8.1
Δδ/ΔT	-	-4.4	-4.8	-6.4	-	-6.8	-4.6	-0.3	-	-6.6	-5.0	-	-5.0

C)

EX13[a]	G1	G2	Y3	G4	L5	P6	Y7	T8	T9	G10	K11	L12	P13	Y14
dαN(i,i+1)														
dαN(i,i)														
dNN(i,i+1)														
$^3J_{NH\alpha}$[c]		11.4	7.3	#	7.0	-	6.7	7.6	7.1	#	7.0	6.7	-	6.8
Δδ/ΔT		-4.5	-6.8	-5.6	-6.1	-	-8	-4.6	-4.8	-5.3	-5.4	-7.2	-	-6.2

D)

EX13[b]	G1	G2	Y3	G4	L5	P6	Y7	T8	T9	G10	K11	L12	P13	Y14
dαN(i,i+1)														
dαN(i,i)														
dNN(i,i+1)														
dαN(i,i+2)														
$^3J_{NH\alpha}$[c]		11.5	7.0	12.0	6.5	-	6.3	#	7.5	12	8.0	#	-	7.6
Δδ/ΔT		-4.3	#	-5.2	-4.8	-	-4.6	#	#	-5.2	-5.0	#	-	-3.4

[a] spectra recorded in H_2O/D_2O 90/10 at 298K

[b] spectra recorded in TFE-$_{d3}$/H_2O 80/20 at 298K

[c] The J values for Gly residues are the sum of J_{AX} and J_{BX}, [d] # (not determined)

FIGURE 12: Summary of NMR parameters of EX4 peptide: (A) in water and (B) in TFE-d_3/H_2O 70/30; EX13 peptide: (C) in water and (D) in TFE-d_3/H_2O 70/30. The summary includes sequential and medium range NOEs, the ^3J coupling constants (Hz), and temperature coefficients ($\Delta\delta/\Delta T$, ppb/K). The NOE intensities are reflected by the thickness of the lines. When an unambiguous assignment was not possible due to peak overlap, the NOEs are drawn with gray lines.

lished data). Furthermore, some of them exhibit the same fractal organization previously found for elastin (*32*). Consequently, it is possible to know which specific sequences in the parent protein are responsible for specific functions, such as self-assembly of tropoelastin, and also their contributions to the entropic elasticity. Accordingly, the reductionist approach we used in the present paper is a posteriori validated.

Of particular interest, as far as the mechanism of elasticity of elastin is concerned, is the finding that in aqueous solution the dominant conformation is apparently the PPII often in equilibrium with the so-called "unordered" state. It can be rationalized within the framework of the proposal (*53*−*55*, *74*), that PPII is a significant contributor to the conformational ensemble in flexible, unordered polypeptides. In fact, recently a new picture of unordered conformations emerged from the analysis of unfolded proteins and unordered peptides that points to more restricted conformational sampling in the unordered state with a limited range of accessible conformations. Many spectroscopic studies (CD, VCD, ROA) and molecular dynamics simulations propose that short stretches of 2−5 residues in PPII are the most favored conformation in solution for unordered and unfolded peptides. Furthermore, the unordered form is constituted not only by PPII-helical

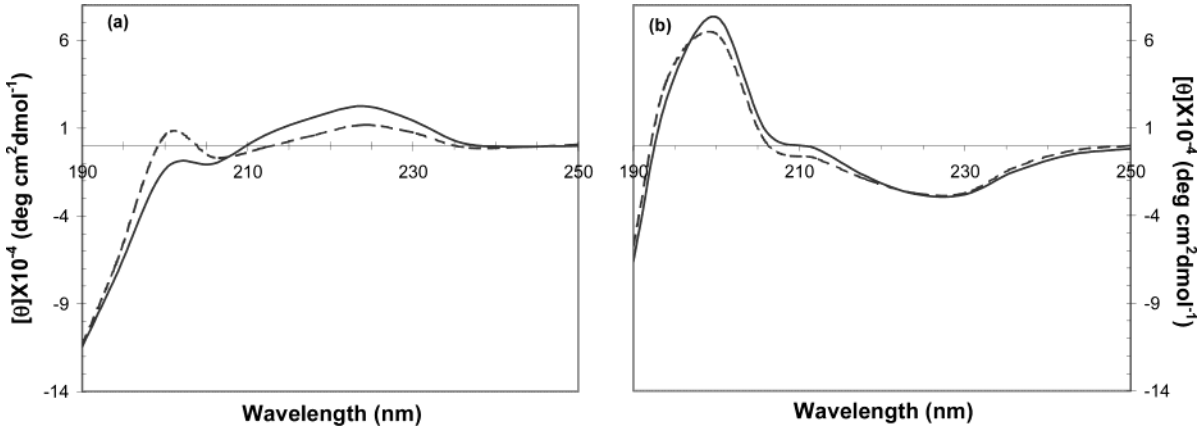

FIGURE 13: CD spectra of EX13 peptide in water (a) and in TFE (b) recorded at different temperatures: (—) at 0 °C, (−− −− —) at 25 °X, (- - -) at 70 °C.

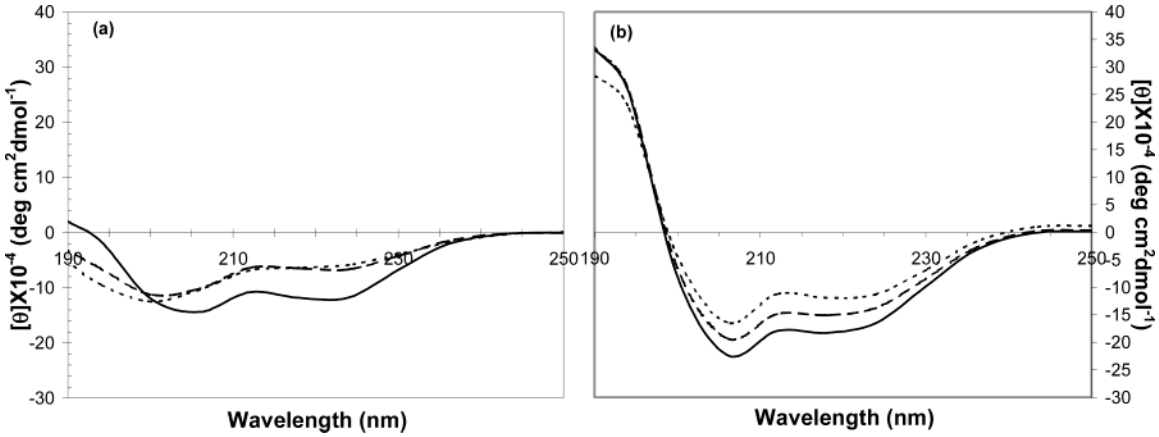

FIGURE 14: CD spectra of EX19 peptide in water (a) and in TFE (b) recorded at different temperatures: (—) at 0 °C, (−− −− —) at 25 °C, (- - -) at 70 °C.

stretches with three or more residues but also by conformers in which individual residues are in PPII, α-, or β-regions of the Ramachandran map, rapidly interconverting. There is some evidence indicating that PPII is at the global energy minimum for peptides in water (*53* and refs therein).

In TFE, in contrast, folded conformations, such as type I and type II β-turns are found together with unordered conformations. Because the polarity of the microenviroment might be intermediate between water and TFE, we can suggest a conformational equilibrium for elastin, comprising PPII, β-turns, and unordered conformations.

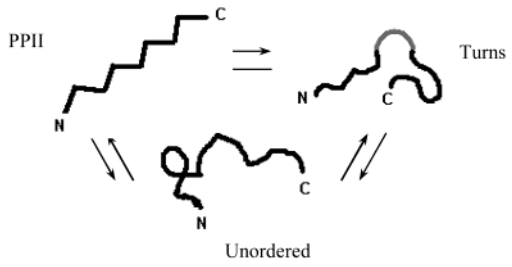

Each of the three terms at the equilibrium should comprise, on their own, additional internal fluctuations. Such is, for example, the case of PPII, where most probably the trans-conformational transitions involve the entire upper left region of the Ramachandran map, that is, the region of the (quasi) extended conformation, including also β-strands. Similarly, the comprehensive word β-turns is used to refer to fluctuations around the energy minimum of isolated β-turns and also equilibria such as type I ⇄ type II, well-known in the literature. These latter structures have been proposed as a common structure in elastin (*75*), and are central to the "sliding β-turns" model proposed by Tamburro as an explanation for elastin elasticity (*14*, *76*). Furthermore, PPII is an ubiquitous structure in elastomeric proteins, such as gluten proteins (*77*, *78*), titin, and abductin (*56*, and references therein). As a native, relaxed state at high entropy is essential for the expression of elasticity according to the classical theory of rubber elasticity, a pivotal role in this context is played by the PPII flexibility. In fact, the main peculiarity of PPII lies in its high flexibility undoubtedly due to the absence of intrachain hydrogen bonds. Accordingly, the possibility that PPII is involved, as suggested above, in multiconformational equilibria such as PPII/unordered/β-turns, should conceivably increase the entropy of the relaxed state and therefore allow the expression of elasticity.

The results reported in this paper strongly support the general equilibrium: extended ⇄ folded, considered in the Tamburro model to be the source of the high entropy of elastin relaxed state (*12*, *14*).

They also allow us to develop a unified model of elasticity by incorporating previous results and models from our group and other laboratories. Of particular note is the β-spiral structure proposed (*79*) for the repeating sequence -VPGVG- and characterized by a helical arrangement of type II β-turns,

A)

EX19[a]	G1	V2	V3	S4	P5	E6	A7	A8	A9	K10	A11	A12	A13	K14	A15	A16	K17	Y18
dαβ(i,i+3)																		
dNN(i,i+2)																		
dNN(i,i+1)																		
$^3J_{NH\alpha}$	-	7.4	7.8	6.3	-	6.2	#	5.1	#	#	#	#	5.4	#	#	#	#	8.2
Δδ/ΔT	-	-5.0	-7.7	-8.8	-	-6.2	-4.8	-8.5	-5.2	#	#	#	-4.9	#	#	#	#	-6.1

B)

EX19[b]	G1	V2	V3	S4	P5	E6	A7	A8	A9	K10	A11	A12	A13	K14	A15	A16	K17	Y18
dαβ(i,i+3)																		
dNN(i,i+2)																		
dαN(i,i+2)																		
dNN(i,i+1)																		
$^3J_{NH\alpha}$	-	7.5	#[c]	#	-	5.1	5.2	#	4.4	4.0	4.0	4.4	5.1	5.6	#	5.7	#	#
Δδ/ΔT	-	-4.7	#	#	#	#	-2.4	#	-5.2	#	-5.0	-4.9	-4.4	-4.9	#	#	#	#

[a] spectra recorded in H_2O/D_2O 90/10 at 298K

[b] spectra recorded in TFE-$_{d3}$/H_2O 70/30 at 298K

[c] # (not determined)

FIGURE 15: Summary of NMR parameters of EX19 peptide: (A) in water and (B) in TFE-d_3/H_2O 70/30. The summary includes sequential and medium range NOEs, the ^3J coupling constants (Hz), and temperature coefficients ($\Delta\delta/\Delta T$, ppb/K). The NOE intensities are reflected by the thickness of the lines. When an unambiguous assignment was not possible due to peak overlap, the NOEs are drawn with gray lines.

having -PG- at the corners. In the segments containing -VG-, suspended between β-turns, large-amplitude, low-frequency motions (librations) can occur giving rise to the high entropy of the relaxed state. The decrease in amplitude of the librations on extension causes a decrease in the entropy of the dipeptide segment, providing the driving force for returning to the relaxed state (*80*). While this model provides a probable mechanistic description for local regions of elastin, essentially those comprising PG segments, it seems not to explain the elasticity of the whole protein. In fact, recent molecular dynamics simulations (*81*) show that short stretches of β-spiral are indeed possible, but they are transient structures quickly interconverting into isolated β-turns and extended structures, such as β-strands. The presence of β-strands in elastin in the solid state has been shown (*9*, *82*). Accordingly, the β-spiral model of Urry can be incorporated into the general equilibrium folded $\rightleftarrows$ extended as one of the different rapidly interconverting folded structures. While the librational motions are undoubtly contributing to the internal chain dynamics, they are nevertheless acting not only outside the β-turns, but also inside the hydrogen-bonded cycles (*83*), constituting an important conformational fluctuation when the β-turns are isolated.

The folded $\rightleftarrows$ extended equilibrium was previously modeled for several short, repeating sequences of elastin in explicit aqueous solvent in terms of nonlinear dynamic systems (*84*). In the relaxed state, the dynamics of the formation and breaking of intramolecular hydrogen bonds was found to be characteristic of a chaotic Brownian-like, intramolecular motion. When the simulation was performed on a stretched peptide sequence, a different dynamical behavior was obtained, indicating a transition to low entropy, quasiperiodic soliton-like motion. The results presented in the current paper allow us to interpret these theoretical findings in the context of the entire protein. Because folded/extended conformations were found in all exons of elastin (except those of KA type), one can reasonably infer that the same dynamic picture holds for the intact protein in the relaxed/stretched state.

A final comment concerns the role played by the aqueous solvent and the hydrophobic mechanism of elasticity proposed by Gosline (*85*). In our model, the aqueous solvent functions to facilitate the folded $\rightleftarrows$ extended conformational equilibria, giving rise to a noticeable internal main chain dynamics. In the model proposed by Gosline, at low extensions the absorption of water onto exposed hydrophobic groups causes a large decrease in entropy, contributing to the restoring elastomeric force. Molecular dynamics simulations (*81*) appear to support this solvent-entropy mechanism. In terms of nonlinear dynamic systems theory, the Gosline mechanism can be incorporated in our dynamical model. In fact, diffusive (chaotic) motions of bulk water in the relaxed maximum entropy state would be substituted by vibrational (quasiperiodic?) motions of clathrate water in the extended state. However, previous measurements (*86*) have clearly demonstrated that elastin behaves as an ideal rubber even in dimethyl sulfoxide. This means that elastin's elasticity does not specifically depend on the aqueous solvent, but rather on the presence of a polar solvent, which would act as a plasticizer, favoring trans-conformational equilibria. Accordingly, internal main chain dynamics should be, at least in part, at the origin of the elasticity.

ACKNOWLEDGMENT

We thank Dr. Robert P. Mecham (Washington University, St. Louis, MO) for critical reading of the manuscript.

REFERENCES

1. Debelle, L., and Tamburro, A. M. (1999) Elastin: molecular description and function. *Int. J. Biochem. Cell. Biol. 31*, 261−272.
2. Gibson, M. A., Hatzinikolas, G., Kumaratilake, J. S., Sandberg, L. B., Nicholl, J. K., Sutherland, G. R., and Cleary, E. G. (1996) Further characterization of proteins associated with elastic fiber microfibrils including the molecular cloning of MAGP-2 (MP25). *J. Biol. Chem. 271*, 1096−1103.
3. Kielty, C. M., Baldock, C., Lee, D., Rock, M. J., Ashworth, J. L., and Shuttleworth, C. A. (2002) Fibrillin: from microfibril assembly to biomechanical function. *Philos. Trans. R. Soc. London B. Biol. Sci. 357*, 207−217.
4. Handford, P. A., Downing, A. K., Reinhardt, D. P., and Sakai, L. Y. (2000) Fibrillin: from domain structure to supramolecular assembly. *Matrix Biol. 19*, 457−470.
5. Gosline, J. M., (1987) Structure and mechanical properties of rubberlike proteins in animals. *Rubber Chem. Technol. 60*, 417−438.
6. Tatham, A. S., and Shewry, P. R. (2000) Elastomeric proteins: biological roles, structures and mechanisms. *Trends Biochem. Sci. 25*, 567−571.
7. Martino, M., Perri, T., and Tamburro, A. M. (2002) Elastin-based biopolymers: chemical synthesis and structural characterization of linear and cross-linked poly(OrnGlyGlyOrnGly), *Macromol. Biosci. 7*, 319−328.
8. Tamburro, A. M., Guantieri, V., Daga-Gordini, D., Abatangelo, D. (1977). Conformational transitions of α-elastin. *Biochim. Biophys. Acta 492*, 370−376.
9. Debelle, L., Alix, A. J., Jacob, M. P., Huvenne, J. P., Berjot, M., Sombret, B., and Legrand, P. (1995) Bovine elastin and kappa-elastin secondary structure determination by optical spectroscopies. *J. Biol. Chem. 270*, 26099−26103.
10. Urry, D. W. (1983) What is elastin; what is not. *Ultrastruct. Pathol. 4*, 227−251.
11. Long, M. M., Rapaka, R. S., Volpin, D., Pasquali-Ronchetti, I., and Urry, D. W. (1980) Spectroscopic and electron micrographic studies on the repeat tetrapeptide of tropoelastin, (Val-Pro-Gly-Gly)n. *Arch. Biochem. Biophys. 201*, 445−452.
12. Tamburro, A. M., Guantieri, V., and Daga-Gordini, D. (1992) Synthesis and structural studies of a pentapetide sequence of elastin, Poly (Val-Gly-Gly-Leu-Gly). *J. Biomol. Struct. Dyn. 10*, 441−454.
13. Tamburro, A. M., Guantieri, V., Pandolfo, L., and Scopa. A. (1990) Synthetic fragments and analogues of elastin. II Conformational studies, *Biopolymers 29*, 855−870.
14. Tamburro, A. M. (1990) Order−disorder in the structure of elastin: a synthetic approach in *Elastin: Chemical and Biological Aspects* (Tamburro A. M., and Davidson J. M., Eds.) pp 127−145, Galatina Congedo Editore, Potenza.
15. Urry, D. W. (1988) Entropic elastic processes in protein mechanisms. II. Simple (passive) and coupled (active) development of elastic forces, *J. Protein Chem. 7*, 81−114.
16. Lee, J., Macosko, C. W., and Urry, D. W. (2001) Mechanical properties of cross-linked synthetic elastomeric polypentapeptides. *Macromolecules 34*, 5968−5974.
17. McMillan, R. A., and Conticello, V. P. (2000) Synthesis and characterization of elastin-mimetic protein gels derived from a well-defined polypeptide precursor. *Macromolecules 33*, 4809−4821.
18. McMillan, R. A., Lee, T. A. T., and Conticello, V. P. (1999) Rapid assembly of synthetic genes encoding protein polymers. *Macromolecules 3*, 3643−3648.
19. Martino, M., Bavoso, A., Guantieri, V., Coviello, A., and Tamburro A. M. (2000) On the occurrence of polyproline II structure in elastin. *J. Mol. Struct. 519*, 173−189.
20. Indik, Z., Abrams, W. R., Kucich, U., Gibson, C. W., Mecham, R. P., and Rosenbloom, J. (1990) Production of recombinant human tropoelastin: characterization and demonstration of immunologic and chemotactic activity. *Arch. Biochem. Biophys. 280*, 80−86.
21. Martin, S. L., Vrhovski, B., and Weiss, A. S. (1995) Total synthesis and expression in *Escherichia coli* of a gene encoding human tropoelastin. *Gene 154*, 159−166.
22. Vrhovski, B., Jensen, S., and Weiss, A. S. (1997) Coacervation characteristics of recombinant human tropoelastin. *Eur. J. Biochem. 250*, 92−98.
23. Debelle, L., and Alix, A. J. P. (1995) Optical spectroscopic determination of bovine tropoelastin molecular model. *J. Mol. Struct. 348*, 321−324.
24. Indik, Z., Yeh, H., Ornstein-Goldstein, N., Sheppard, P., Anderson, N., Rosenbloom, J. C., Peltonen, L., and Rosenbloom, J. (1987) Alternative splicing of human elastin mRNA indicated by sequence analysis of cloned genomic and complementary DNA. *Proc. Natl. Acad. Sci. U.S.A. 84*, 5680−5604.
25. Rosenbloom, J., Abrams, W. R., and Mecham, R. P. (1993) Extracellular matrix 4: the elastic fiber. *FASEB J. 7*, 1208−1218.
26. Tamburro, A. M., Daga-Gordini, D., Guantieri V., and De Stradis A. (1994) On the molecular and the supramolecular structure of elastin in *Chemistry and Properties of Biomolecular Systems* (Russo, N., Anastassopoulou, S., and Barone, G., Eds.) Vol. 2, pp 389−403, Kluwer, Dordrecht.
27. Tamburro, A. M., De Stradis, A., D'Alessio, L. (1995) Fractal aspects of Elastin supramolecular organization. *J. Biomol. Struct. Dyn. 12*, 1161−1172.
28. D'Alessio, L., Tamburro A. M., and De Stradis A. (1999) Observation of fractal structures in the supramolecular organization of protein molecules in *Fractals in Engineering, Proceedings*, pp 130−137.
29. Tamburro, A. M. (1995) The supramolecular structures of Elastin and related synthetic polypeptides: Scale invariant weaving in *Macrocyclic and Supramolecular Chemistry in Italy* (Savelli, G., Ed.) pp 265−268, Centro Stampa Università di Perugia, Italy.
30. Bressan G. M., Argos, P., and Stanley, K. K. (1987) Repeating structure of chick tropoelastin revealed by complementary DNA cloning. *Biochemistry 26*, 1497−1503.
31. Long, M. M., King, V. J., Prasad, K. U., and Urry, D. W. (1988) Chemotaxis of fibroblasts toward nonapeptide of elastin. *Biochim. Biophys. Acta 968*, 300−311.
32. Castiglione-Morelli, M. A., Bisaccia, F., Spisani, S., De Biasi, M., Traniello, S., and Tamburro, A. M. (1997) Structure−activity relationships for some elastin-derived peptide chemoattractants. *J. Pept. Res. 49*, 492−499.
33. Bisaccia, F., Castiglione-Morelli, M. A., Spisani, S., Ostuni, A., Serafini-Fracassini, A., Bavoso, A., and Tamburro, A. M. (1998) The amino acid sequence coded by the rarely expressed exon 26A of human elastin contains a stable beta-turn with chemotactic activity for monocytes. *Biochemistry 37*, 11128−11135.
34. Ostuni, A., Lograno, M. D, Gasbarro, A. R, Bisaccia, F., and Tamburro, A. M. (2002) Novel properties of peptides derived from the sequence coded by exon 26A of human elastin. *Int. J. Biochem. Cell. Bio. 34*, 130−135.
35. Brassart, B., Fuchs, P., Huet, E., Alix, A. J., Wallach, J., Tamburro, A. M., Delacoux, F., Haye, B., Emonard, H., Hornebeck, W., and Debelle, L. (2001) Conformational dependence of collagenase (matrix metalloproteinase-1) upregulation by elastin peptides in cultured fibroblasts. *J. Biol. Chem. 276*, 5222−5227.
36. Foster, J. A., Bruenger, E., Rubin, L., Imberman, M., Kagan, H., Mecham, R., and Franzblau C. (1976) Circular dichroism studies of an elastin cross-linked peptide. *Biopolymers 15*, 833−841.
37. Braunschweiler, L., and Ernst, R. R. (1983) Coherence transfer by isotropic mixing: application to proton correlation spectroscopy. *J. Magn. Reson. 53*, 521−528.
38. Bax, A., and Davis, D. G. (1985) Practical aspects of two-dimensional transverse NOE spectroscopy. *J. Magn. Reson. 63*, 207−215.
39. Piotto, M., Saudek, V., and Sklenar, V. (1992) Gradient-tailored excitation for single-quantum NMR spectroscopy of aqueous solutions. *J. Biomol. NMR 2*, 661−665.
40. Wüthrich, K. (1986) *NMR of Proteins and Nucleic Acids*, Wiley, New York.
41. Fischer, S., Dunbrack, R. L., Jr., and Karplus, M. (1994) Cis−trans imide isomerization of the proline dipeptide. *J. Am. Chem. Soc. 116*, 11931−11937.
42. Venkatachalam, C. M., Price, B. J., and Krimm, S. (1975) A theoretical estimate of the energy barriers between stable conformations of the proline dimer. *Biopolymers 14*, 1121−1132.
43. Brown-Augsburger, P., Tisdale, C., Broekelmann, T., Sloan, C., Mecham, R. P., (1995) Identification of an elastin cross-linking domain that joins three peptide chains. Possible role in nucleated assembly. *J. Biol. Chem. 270*, 17778−17783.
44. Bodkin, M. J., and Goodfellow, J. M. (1996) Hydrophobic solvation in aqueous trifluoroethanol solution. *Biopolymers 39*, 43−50.

45. Buck, M. (1998) Trifluoroethanol and colleagues: cosolvents come of age. Recent studies with peptides and proteins. *Q. Rev. Biophys. 31*, 297−355.
46. Reisersen, H., and Rees, A. R. (2000) Trifluoroethanol may form a solvent matrix for assisted hydrophobic interactions between peptide side chains. *Protein Eng. 13*, 739−43.
47. Sreerama, N., and Woody, R. W. (2000) Estimation of protein secondary structure from circular dichroism spectra: comparison of CONTIN, SELCON, and CDSSTR methods. *Anal. Biochem. 287*, 252−60.
48. Sreerama, N., and Woody, R. W. (1993) A self-consistent method for the analysis of protein secondary structure from circular dichroism. *Anal. Biochem. 209*, 32−44.
49. Provencher, S. W., and Glöckner, J. (1981) Estimation of globular protein secondary structure from circular dichroism. *Biochemistry 20*, 33−37.
50. Johnson, W. C., Jr. (1999) Analyzing protein circular dichroism spectra for accurate secondary structures. *Proteins: Struct. Funct. Genet. 35*, 307−312.
51. Perczel, A., Hollósi, M., Sàndor, P., and Fasman, G. D. (1993) The evaluation of type I and type II beta-turn mixtures. Circular dichroism, NMR and molecular dynamics studies. *Int. J. Peptide Protein Res. 41*, 223−236.
52. Drake, A. F., Siligardi, G., and Gibbons, W. A. (1988) Reassessment of the electronic circular dichroism criteria for random coil conformations of poly(L-lysine) and the implications for protein folding and denaturation studies. *Biophys. Chem. 31*, 143−146.
53. Woody, R. W. (1992) Circular dichroism and conformations of unordered polypeptides. *Adv. Biophys. Chem. 2*, 37−79.
54. Shi, Z., Woody, R. W., and Kallenbach, N. R. (2002) Is polyproline II a major backbone conformation in unfolded proteins? *Adv. Protein Chem. 62*, 163−240.
55. Shi, Z., Olson, C. A., Rose, G. D., Baldwin, R. L., and Kallenbach, N. R. (2002) Polyproline II structure in a sequence of seven alanine residues, *Proc. Natl. Acad. Sci. U.S.A. 9*, 9190−9195.
56. Bochicchio, B., and Tamburro, A. M. (2002) Polyproline II structure in proteins: identification by chiroptical spectroscopies, stability, and functions. *Chirality 14*, 782−792.
57. Tiffany, M. L., and Krimm, S. (1968) Circular dichroism of poly-L-proline in an unordered conformation. *Biopolymers 6*, 1767−1770.
58. Ramachandran, G. N., Sasisekharan, V., and Ramakrishnan, C., (1966) Molecular structure of polyglycine II. *Biochim. Biophys. Acta 112*, 168−170.
59. Lotz, B., and Keith, H. D. (1971) The crystal structures of poly-(L-Ala-Gly-Gly-Gly)II and Poly(L-Ala-Gly-Gly)II. *J. Mol. Biol. 61*, 195−200.
60. Kelly, M. A., Chellgren, B. W., Rucker, A. L., Troutman, J. M., Fried, M. G., Miller, A. F., and Creamer, T. P. (2001) Host−guest study of left-handed polyproline II helix formation. *Biochemistry 40*, 14376−14383.
61. Sreerama, N., and Woody, R. W. (1999) Molecular dynamics simulations of polypeptide conformations in water: A comparison of alpha, beta, and poly(pro)II conformations. *Proteins 36*, 400−406.
62. Pappu, R. V., and Rose, G. D. (2002) A simple model for polyproline II structure in unfolded states of alanine-based peptides. *Protein Sci. 11*, 2437−2455.
63. Martino, M., Bavoso, A., Saviano, M., Di Blasio, B., Tamburro, A. M. (1998) Structure and dynamics of elastin building blocks. Boc-LG-OEt, Boc-VGG-OH. *J. Biomol. Struct. Dyn. 15*, 861−874.
64. Wishart, D. S., Sykes, B. D., and Richards, F. M. 1992. The chemical shift index: a fast and simple method for the assignment of protein secondary structure through NMR spectroscopy. *Biochemistry 31*, 1647−1651.
65. Karplus, M. (1959) Contact electron-spin coupling of nuclear magnetic moments. *J. Chem. Phys. 30*, 11−15.
66. Bürgi, R., Pitera, J., and van Gunsteren, W. F. (2001) Assessing the effect of conformational averaging on the measured values of observables. *J. Biomol. NMR, 19*, 305−320.
67. Sharman, G. J., and Searle, M. S. (1998) Cooperative interaction between the three strands of a designed antiparallel β-sheet. *J. Am. Chem. Soc. 120*, 5291−5300.
68. Fiebig, K. M., Schwalbe, H., Buck, M., Smith, L. J., and Dobson, C. M. (1996) Toward a description of the conformations of denatured states of proteins. comparison of a random coil model with NMR measurements. *J. Phys. Chem. 100*, 2661−2666.
69. Creamer, T. P., and Campbell, M. N. (2002) Determinants of the polyproline II helix from modeling studies. *Adv. Protein Chem. 62*, 263−282.
70. Dyson, H. J., Bolinger, L., Feher, V. A., Osterhout, J. J., Yao, J., and Wright, P. (1998) Sequence requirements for stabilization of a peptide reverse turn in water solution—proline is not essential for stability. *Eur. J. Biochem. 255*, 462−471.
71. Makarov, A. A., Lobachov, V. M., Adzhubei, I. A. and Esipova, N. G. (1992) Natural polypeptides in left-handed helical conformation. A circular dichroism study of the linker histones' C-terminal fragments and beta-endorphin. *FEBS Lett. 306*, 63−65.
72. Manning, M. C. and Woody, R. W. (1989) Theoretical study of the contribution of aromatic side chains to the circular dichroism of basic bovine pancreatic trypsin inhibitor. *Biochemistry 28*, 8609−8613.
73. Woody, R. W. and Dunker, A. K. (1996) in *Circular Dichroism and the Conformational Analysis of Biomolecules* (Fasman, G. D., Ed.) pp 109−157, Plenum Press, New York.
74. Rucker, A. L. and Creamer, T. P. (2002) Polyproline II helical structure in protein unfolded states: Lysine peptides revisited. *Protein Sci. 11*, 980−985.
75. Martino, M., Coviello, A. and Tamburro, A. M. (2000) Synthesis and structural characterization of poly (LGGVG), an elastin-like polypeptide. *Int. J. Biol. Macromol. 27*, 59−64.
76. Lelj, F., Tamburro, A. M., Villani, V., Grimaldi, P. and Guantieri, V. (1992) Molecular dynamics study of the conformational behavior of a representative elastin building block: Boc-Gly-Val-Gly-Gly-Leu-Ome. *Biopolymers 32*, 159−170.
77. Blanch, E. W., Kasarda, D. D:, Hecht, L., Nielsen, K. and Barron, L. W. (2003) New Insight into Solution Structures of Wheat Gluten Proteins from Raman Optical Activity. *Biochemistry 42*, 5665−5673.
78. Parrot, I., Huang, P. H., and Khosla, C. (2002) Circular Dichroism and Nuclear Magnetic Resonance Spectroscopic Analysis of Immunogenic Gluten Peptides and Their Analogs. *J. Biol. Chem. 277*, 45572−45578.
79. Venkatachalam, C. M., and Urry, D. W. (1981) Development of a linear helical conformation from its cyclic correlate. β-Spiral model of the elastin poly(pentapeptide) (VPGVG)n. *Macromolecules 14*, 1225−1229.
80. Urry, D. W. (1988) Entropic elastic processes in protein mechanisms. I. Elastic structure due to an inverse temperature transition and elasticity due to internal chain dynamics. *J. Protein Chem. 7*, 1−34.
81. Li, B., Alonso, D. O., Bennion, B. J., and Daggett, V. (2001) Hydrophobic hydration is an important source of elasticity in elastin-based biopolymers. *J. Am. Chem. Soc. 123*, 11991−11998.
82. Debelle, L., Alix, A. J., Wei, S. M., Jacob, M. P., Huvenne, J. P., Berjot, M. and Legrand, P. (1998) The secondary structure and architecture of human elastin. *Eur. J. Biochem. 258*, 533−539.
83. Villani, V., and Tamburro, A. M. (1995) Conformational Modeling of Elastin Tetrapeptide Boc-Gly-Leu-Gly-Gly-Nme by Molecular Dynamics Simulations with Improvements to the Thermalization Procedure. *J. Biomol. Struct. Dyn. 12*, 1173−1202.
84. Villani, V., Tamburro, A. M., and Zaldivar Comenges, J. M. (2000) Conformational chaos and biomolecular instability in aqueous solution. *J. Chem. Soc., Perkin Trans. 2*, 2177−2184.
85. Gosline, J. M. (1978) Hydrophobic interaction and a model for the elasticity of elastin. *Biopolymers 17*, 677−695.
86. Mistrali, A., Volpin, D., Garibaldo, G. B., and Ciferri, A. (1971) Thermodynamics of elasticity in open systems. *Elastin J. Phys. Chem. 75*, 142−149.

BI034837T